BURNS, D. M. & IBALL, J. (1955). *Proc. Roy. Soc.* A, **227**, 200.
COMPTON, A. H. & ALLISON, S. K. (1935). *X-rays in Theory and Experiment.* New York: Van Nostrand.
DIAMOND, R. (1958). *Acta Cryst.* **11**, 129.
HARTREE, D. R. (1952). *Numerical Analysis.* Oxford: Clarendon Press.
KEATING, D. T. & VINEYARD, G. H. (1956). *Acta Cryst.* **9**, 895.
KEATING, D. T. & WARREN, B. E. (1952). *Rev. Sci. Instrum.* **23**, 519.
MILBERG, M. E. (1958). *J. Appl. Phys.* **29**, 64.
MILBERG, M. E. & BRAILSFORD, A. D. (1958). *Acta Cryst.* **11**, 672.
ROSS, P. A. (1928). *J. Opt. Soc. Amer.* **16**, 433.

Acta Cryst. (1959). **12**, 683

The Effect of Segregation on the Diffraction from a Face-Centred Cubic Alloy with Deformation Faults

BY B. T. M. WILLIS

Atomic Energy Research Establishment, Harwell, Berks, England

(*Received* 9 *October* 1958 *and in revised form* 16 *March* 1959)

The Paterson theory of X-ray scattering from a face-centred cubic structure with deformation faults is extended to include the case of a f.c.c. alloy, in which segregation of the alloy components takes place at the faults. The principal effect of segregation is to make the reflexions asymmetrical. It is possible that this asymmetry could be detected in the powder lines of certain cold-worked alloys.

1. Introduction

Suzuki (1952) has suggested a hardening mechanism for face-centred cubic alloys, involving a segregation of solute atoms at deformation stacking faults. Segregation can occur because the crystal structure is close-packed hexagonal in a layer two atoms thick at the stacking fault; the concentration of solute atoms at the fault will therefore differ from the average, when the faulted region is in thermodynamic equilibrium with the surrounding cubic phase. Using this idea Suzuki has explained certain mechanical properties of alloys (see also Cottrell, 1954), but so far no direct evidence for segregation has been obtained. It is possible that such evidence could be provided by X-ray diffraction.

The purpose of this paper is to calculate the nature of the X-ray scattering from a deformation-faulted f.c.c. alloy, in which the alloy composition at the faults differs from that in the cubic matrix. We thus require to extend the treatment of Paterson (1952), dealing with the diffraction from a homogeneous, faulted f.c.c. crystal, to include the case of segregation.

2. Intensity distribution in reciprocal space

(*a*) *General formula*

Fig. 1(*a*) illustrates the stacking sequence of the close-packed (111) layers, with the faulted positions denoted by F, and f_1, f_2 representing the scattering powers averaged over the atoms in the two kinds of layer. When several faults occur in succession, the c.p.h. structure is developed only at the boundaries of the set, so that segregation takes place only at the kinks in the 'stacking line'.

The theory developed in this section assumes that there is no change of layer spacing accompanying segregation. The extension of the theory to include both change of scattering power and of spacing is considered in the Appendix, but it is shown there that the simpler theory of this section is adequate for most cases.

We make the usual assumption that faulting is restricted to one set of (111) planes only: the limitations imposed by this assumption have been considered by Willis (1958).

At first, the treatment follows very closely that given by Warren & Warekois (1955) for the problem of deformation-faulting without segregation.

It is convenient to choose hexagonal axes $\mathbf{A}_1$, $\mathbf{A}_2$, $\mathbf{A}_3$, with $\mathbf{A}_1$, $\mathbf{A}_2$ in the (111) plane and $\mathbf{A}_3$ normal to this plane. If $\mathbf{a}_1$, $\mathbf{a}_2$, $\mathbf{a}_3$ are the cubic axes of the unfaulted structure, then

$$\left.\begin{aligned} \mathbf{A}_1 &= -\mathbf{a}_1/2+\mathbf{a}_2/2 \\ \mathbf{A}_2 &= -\mathbf{a}_2/2+\mathbf{a}_3/2 \\ \mathbf{A}_3 &= \mathbf{a}_1/3+\mathbf{a}_2/3+\mathbf{a}_3/3\,. \end{aligned}\right\} \qquad (1)$$

Similar equations relate the corresponding hexagonal H_1, H_2, H_3 and cubic hkl indices:

$$\left.\begin{aligned} H_1 &= -h/2+k/2 \\ H_2 &= -k/2+l/2 \\ H_3 &= h/3+k/3+l/3\,. \end{aligned}\right\} \qquad (1a)$$

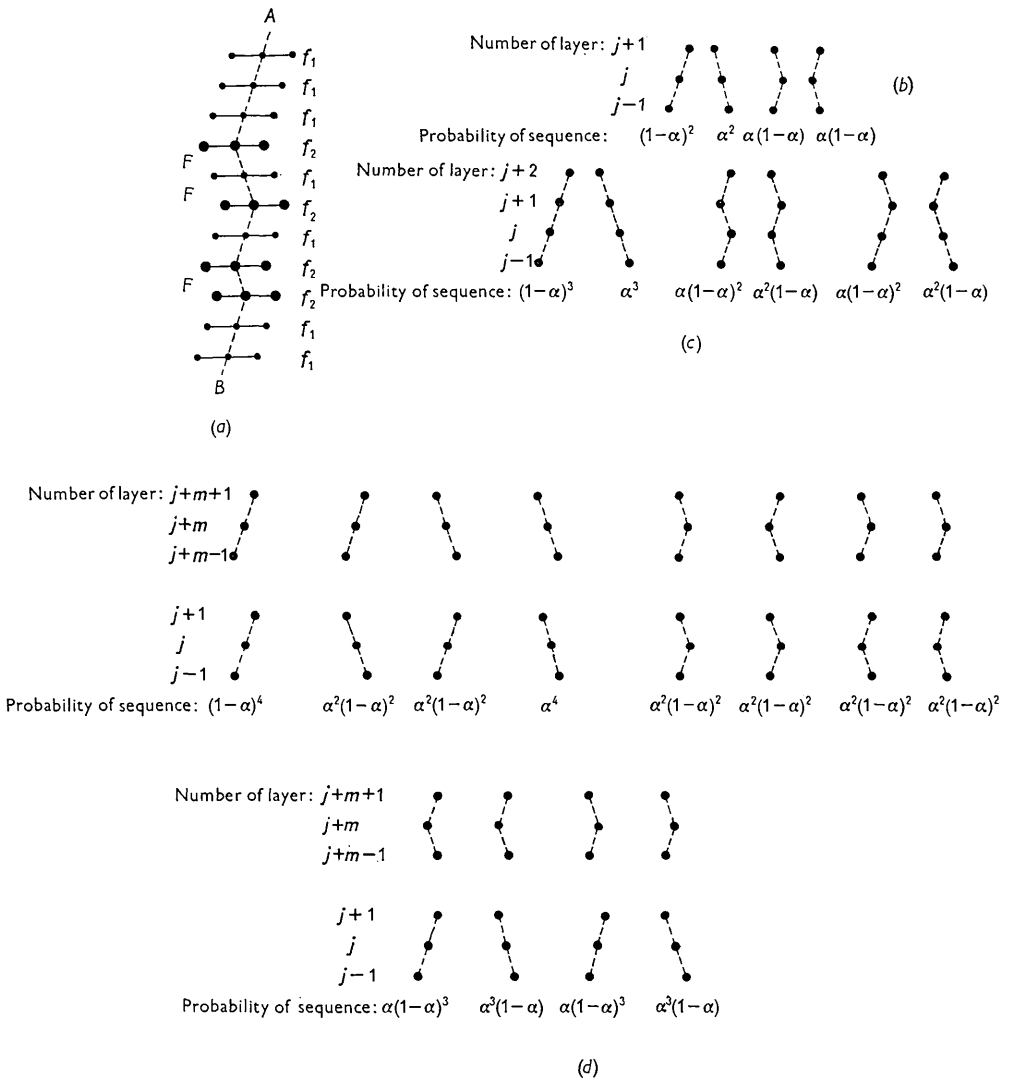

Fig. 1. (*a*) Diagram illustrating stacking sequence of (111) layers. Faulted positions are denoted F, and the average scattering powers of the atoms in the two kinds of layer are denoted f_1, f_2. The 'stacking line' is the broken line AB. (*b*) Different types of sequence for three successive layers. (*c*) Different types of sequence for four successive layers. (*d*) Different types of sequence for the six layers $j-1$, j, $j+1$, $j+m-1$, $j+m$, $j+m+1$, where $m \geq 2$.

In the presence of faulting $\mathbf{A}_3$ is not a repetition vector of the lattice, and so H_3 is not necessarily integral.

Let $\mathbf{r}_{m_1m_2m_3}$ be the position vector of the atom m_1m_2 in layer m_3, i.e.

$$\mathbf{r}_{m_1m_2m_3} = m_1\mathbf{A}_1+m_2\mathbf{A}_2+m_3\mathbf{A}_3+\delta_{m_3}\,, \qquad (2)$$

where δ_{m_3} is a vector which depends on m_3 and gives the change in $\mathbf{r}$ due to the presence of faults. (δ_{m_3} can be written $\frac{1}{3}n_{m_3}(\mathbf{A}_1-\mathbf{A}_2)$, where n_{m_3} is an integer depending on m_3.) The diffracted intensity I is then

$$I = I_e \sum_{m_1m_2m_3} \sum_{m_1'm_2'm_3'} f_{m_1m_2m_3}f_{m_1'm_2'm_3'} \times \exp\frac{2\pi i}{\lambda}(\mathbf{S}-\mathbf{S}_0)\cdot(\mathbf{r}_{m_1'm_2'm_3'}-\mathbf{r}_{m_1m_2m_3})\,, \qquad (3)$$

where $\mathbf{S}_0$, $\mathbf{S}$ are unit vectors along the incident and scattered directions, λ the incident wavelength and I_e the scattered intensity per electron. Substituting (2) into (3) gives:

$$I = I_e \sum_{m_1m_2m_3} \sum_{m_1'm_2'm_3'} f_{m_1m_2m_3}f_{m_1'm_2'm_3'} \times \exp\left\{\frac{2\pi i}{\lambda}(\mathbf{S}-\mathbf{S}_0)\cdot[(m_1'-m_1)\mathbf{A}_1+(m_2'-m_2)\mathbf{A}_2 +(m_3'-m_3)\mathbf{A}_3+\delta_{m_3'}-\delta_{m_3}]\right\}. \qquad (4)$$

The average scattering power of an atom depends on m_3 only and can be written f_{m_3}. Further if we consider the unfaulted crystal to be in the form of a parallelepiped, and neglect a small term corresponding to

weak diffuse scattering and arising from the disordered distribution of atoms in the (111) plane, (4) becomes:

$$I = I_e \frac{\sin^2\left[\frac{\pi}{\lambda}(\mathbf{S}-\mathbf{S}_0)\cdot N_1\mathbf{A}_1\right]}{\sin^2\left[\frac{\pi}{\lambda}(\mathbf{S}-\mathbf{S}_0)\cdot\mathbf{A}_1\right]} \frac{\sin^2\left[\frac{\pi}{\lambda}(\mathbf{S}-\mathbf{S}_0)\cdot N_2\mathbf{A}_2\right]}{\sin^2\left[\frac{\pi}{\lambda}(\mathbf{S}-\mathbf{S}_0)\cdot\mathbf{A}_2\right]} \times \sum_{m_3}\sum_{m_3'} f_{m_3}f_{m_3'} \exp\left\{\frac{2\pi i}{\lambda}(\mathbf{S}-\mathbf{S}_0) \cdot[(m_3'-m)\mathbf{A}_3+\boldsymbol{\delta}_{m_3'}-\boldsymbol{\delta}_{m_3}]\right\}. \quad (5)$$

Here N_1, N_2 are the number of atoms along the $\mathbf{A}_1$, $\mathbf{A}_2$ directions. If the coefficient of the summation is denoted by Φ^2 and $\boldsymbol{\delta}_{j+m}-\boldsymbol{\delta}_j$ by Δ_m, where j, $j+m$ refer to the jth, $j+m$th layers, then the summations can be separated and written as:

$$I = \Phi^2 \sum_{m=-N}^{N} N_m \langle f_j f_{j+m} \exp\left[\frac{2\pi i}{\lambda}(\mathbf{S}-\mathbf{S}_0)\cdot\Delta_m\right]\rangle_{\text{av.}} \times \exp\left[\frac{2\pi i}{\lambda}(\mathbf{S}-\mathbf{S}_0)\cdot m\mathbf{A}_3\right].$$

N is the total number of layers and N_m the number of layers with an mth neighbouring layer (i.e. $N_m = N-|m|$). $(\mathbf{S}-\mathbf{S}_0)/\lambda$ can be expressed in terms of the basis vectors $\mathbf{B}_1$, $\mathbf{B}_2$, $\mathbf{B}_3$ reciprocal to $\mathbf{A}_1$, $\mathbf{A}_2$, $\mathbf{A}_3$, using h_1, h_2, h_3 as continuous co-ordinates:

$$(\mathbf{S}-\mathbf{S}_0)/\lambda = h_1\mathbf{B}_1+h_2\mathbf{B}_2+h_3\mathbf{B}_3.$$

Putting

$$\frac{2\pi}{\lambda}(\mathbf{S}-\mathbf{S}_0).\Delta_m = \theta_m$$

we obtain the following general formula for the diffracted intensity:

$$I = \Phi^2 \sum_{m=-N}^{N} N_m \langle f_j f_{j+m} \exp i\theta_m\rangle_{\text{av.}} \exp 2\pi i m h_3. \quad (6)$$

(*b*) *Evaluation of* $\langle f_j f_{j+m} \exp i\theta_m\rangle_{\text{av.}}$

It remains to evaluate $\langle f_j f_{j+m} \exp i\theta_m\rangle_{\text{av.}}$. This can be written in the form

$$\langle f_j f_{j+m} \exp i\theta_m\rangle_{\text{av.}} = P_{11}f_1^2\langle\exp i\theta_m\rangle_{11} + 2P_{12}f_1f_2\langle\exp i\theta_m\rangle_{12} + P_{22}f_2^2\langle\exp i\theta_m\rangle_{22}, \quad (7)$$

where P_{11}, P_{12}, P_{22} are the probabilities that layers j, $j+m$ have atoms of average scattering power f_1 and f_1, f_1 and f_2, f_2 and f_2, and $\langle\exp i\theta_m\rangle_{11}\ldots$ are the corresponding values of $\langle\exp i\theta_m\rangle_{\text{av.}}$ for all such pairs of layers.

(i) $m = 0$

For $m = 0$, $\theta_m = 0$ and $\langle\exp i\theta_m\rangle = 1$. Further, $P_{12} = 0$, and P_{11}, P_{12} are the probabilities that a given layer j has scattering power f_1, f_2 respectively; these probabilities can be readily found from Fig. 1(*b*), showing four different sequences for the layers $j-1$, j, $j+1$. The stacking line is shown as a broken line, and the jth layer is f_1-type in the first pair of sequences and f_2-type in the last pair. Clearly, $P_{11} = \alpha^2+(1-\alpha)^2$ and $P_{22} = 2\alpha(1-\alpha)$, where α is the faulting parameter, i.e. the probability that an arbitrarily chosen layer is faulted.

Substituting these P values into (7) gives:

$$\langle f_j f_{j+m} \exp i\theta_m\rangle = f_1^2(1-2\alpha+2\alpha^2)+f_2^2(2\alpha-2\alpha^2). \quad (8)$$

(ii) $m = 1$

P_{11} and P_{22} are the probabilities that neighbouring layers j, $j+1$ are both f_1-type and both f_2-type, and P_{12} is the probability that j is f_1-type and $j+1$ is f_2-type. We must now consider the six sequences in Fig. 1(*c*). P_{11} is the sum of the probabilities of the first pair of sequences, P_{22} the sum of the next pair, and P_{12} the sum of the last pair. Thus

$$P_{11} = 1-3\alpha+3\alpha^2, \quad P_{22} = P_{12} = \alpha-\alpha^2.$$

Further, $\langle\exp i\theta_m\rangle$ can be written

$$\langle\exp i\theta_m\rangle = (1-\alpha')\exp 2\pi i\left(\frac{-h_1+h_2}{3}\right) + \alpha'\exp 2\pi i\left(\frac{h_1-h_2}{3}\right), \quad (9)$$

where α' is the probability of a fault between the jth, $j+1$th layers. From Fig. 1(*c*) we see that

$\alpha' = \alpha^3/(1-3\alpha+3\alpha^2)$, if layer j is f_1-type and layer $j+1$ is f_1-type,

$= 1-\alpha$, if layer j is f_2-type and layer $j+1$ is f_2-type,

$= \alpha$, if layer j is f_1-type and layer $j+1$ is f_2-type.

$\langle\exp i\theta_m\rangle_{11}$, $\langle\exp i\theta_m\rangle_{22}$, $\langle\exp i\theta_m\rangle_{12}$ are then given by (9) using the appropriate value of α'.

There is appreciable intensity only for h_1, h_2 = integers H_1, H_2 (see equation (5), taking N_1, $N_2 \gg 1$). For the reflexions having $H_1-H_2 = 3M$ (M integral), (7) and (9) give

$$\langle f_j f_{j+m} \exp i\theta_m\rangle = f_1^2[1+4\alpha(1-\alpha)\beta+\alpha(1-\alpha)\beta^2], \quad (10)$$

where $\beta = f_2/f_1-1$; and for the reflexions having $H_1-H_2 = 3M\pm1$

$$\langle f_j f_{j+m} \exp i\theta_m\rangle = -f_1^2 E \exp\pm i\varepsilon, \quad (11)$$

where

$$\left.\begin{aligned} E\cos\varepsilon &= \tfrac{1}{2}[1+4\alpha(1-\alpha)\beta+\alpha(1-\alpha)\beta^2] \\ \text{and} \quad E\sin\varepsilon &= \tfrac{1}{2}\sqrt{3}(1-2\alpha)[1-\alpha(1-\alpha)\beta^2] \end{aligned}\right\}. \quad (11a)$$

(iii) $m \geq 2$

To evaluate the P's we must consider the twelve sequences in Fig. 1(*d*); P_{11} is the sum of the prob-

abilities of the first four, P_{22} of the second four, and P_{12} of the last four. Thus $P_{11} = (1-2\alpha+2\alpha^2)^2$, $P_{22} = 4\alpha^2(1-\alpha)^2$ and $P_{12} = 2\alpha(1-\alpha)(1-2\alpha+2\alpha^2)$.

To determine $\langle \exp i\theta_m \rangle$ we write it as

$$\langle \exp i\theta_m \rangle = \langle \exp i\theta_{0-1} \rangle \langle \exp i\theta_{1-2} \rangle \langle \exp i\theta_{2-3} \rangle \ldots , \quad (12)$$

where $\langle \exp i\theta_{0-1} \rangle$, $\langle \exp i\theta_{1-2} \rangle \ldots$ are the average values of $\exp i\theta$ between layers j and $j+1$, $j+1$ and $j+2 \ldots$. If α'' is the probability of a fault between any pair of neighbouring layers in the sequence j to $j+m$, then for the pairs $j, j+1$ and $j+m-1$, $j+m$ (see Fig. 1(*d*) or Fig. 1(*b*))

$$\begin{aligned} \alpha'' &= \alpha^2/(1-2\alpha+2\alpha^2), && j \text{ and } j+m \ f_1\text{-type}, \\ &= \tfrac{1}{2}, && j \text{ and } j+m \ f_2\text{-type}. \end{aligned}$$

For all other pairs $\alpha'' = \alpha$, independent of f_j, f_{j+m}. The individual averages on the r.h.s. of equation (12) can now be expressed by equation (9) with α' replaced by the appropriate value of α''. Substituting the different values of $\langle \exp i\theta_m \rangle$ and P into (7) finally gives for the $3M$ reflexions:

$$\langle f_j f_{j+m} \exp i\theta_m \rangle = f_1^2[1+4\alpha(1-\alpha)\beta+4\alpha^2(1-\alpha)^2\beta^2]; \quad (13)$$

and for the $3M \pm 1$ reflexions

$$\langle f_j f_{j+m} \exp i\theta_m \rangle = f_1^2(-Z \exp \pm i\gamma)^{m-2} D \exp \pm i\delta, \quad (14)$$

where

$$\left.\begin{aligned} Z^2 &= 1-3\alpha+3\alpha^2, \\ \tan\gamma &= \sqrt{3}(1-2\alpha), \\ D\cos\delta &= -\tfrac{1}{2}+3\alpha-3\alpha^2, \\ D\sin\delta &= \tfrac{1}{2}\sqrt{3}(1-2\alpha)[1+2\alpha(1-\alpha)\beta]. \end{aligned}\right\} \quad (14a)$$

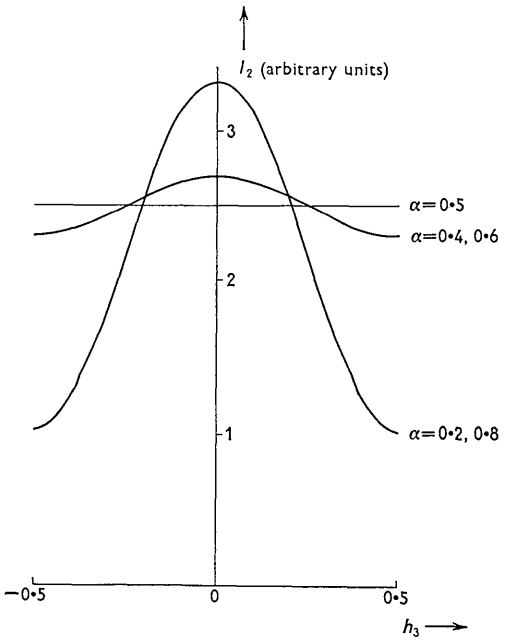

Fig. 2. Dependence of diffuse intensity on h_3 for different values of α.

For $m = -1$, equations (10), (11) apply with $\pm$ in (11) replaced by $\mp$; similarly (13), (14) apply for $m \leq -2$ with $\pm$ in (14) replaced by $\mp$.

(*c*) *Intensity of reflexions having* $H_1-H_2 = 3M$

Substituting (8), (10), (13) into (6) gives

$$I = I_1+I_2$$

where

$$I_1 = f_1^2[1+4\alpha(1-\alpha)\beta + 4\alpha^2(1-\alpha)^2\beta^2] \sum_{m=-N}^{N} (N-|m|)\exp 2\pi i m h_3$$

and

$$I_2 = 2\alpha(1-\alpha)f_1^2\beta^2 \times [1-2\alpha(1-\alpha)+(1-4\alpha+4\alpha^2)\cos 2\pi h_3].$$

I_1 is a term equivalent to diffraction from a perfect crystal and gives sharp peaks at integral h_3. I_2 is a term giving rise to diffuse intensity; its dependence on h_3 for different values of α is shown in Fig. 2. The maximum integrated diffuse intensity occurs for $\alpha = 0{\cdot}5$; I_2 is then independent of h_3, apart from the form-factor dependence of the quantity $f_1^2\beta^2$.

(*d*) *Intensity of reflexions having* $H_1-H_2 = 3M \pm 1$

Substituting (8), (11), (14) into (6), and carrying out the summation, gives

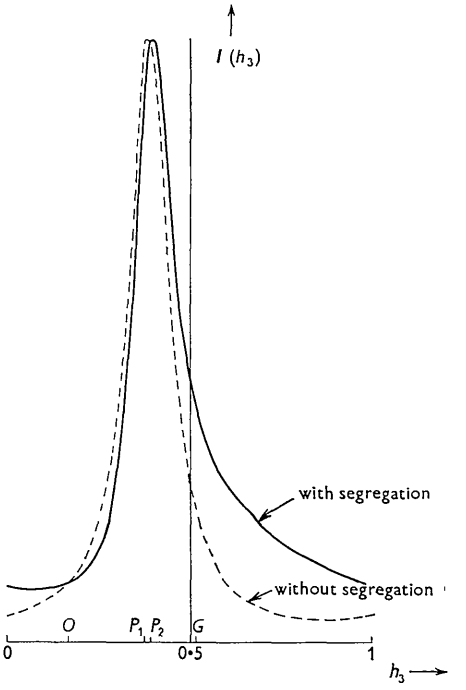

Fig. 3. Curves showing shapes of $3M+1$ diffraction peaks.
– – – $\alpha = 0{\cdot}25$, $\beta = 0$ (faulting without segregation).
—— $\alpha = 0{\cdot}25$, $\beta = 1{\cdot}0$ (faulting with segregation).
Faulting without segregation displaces the peak and the centre of gravity from 0 to P_1; segregation displaces the peak further to P_2 and the centre of gravity to G.

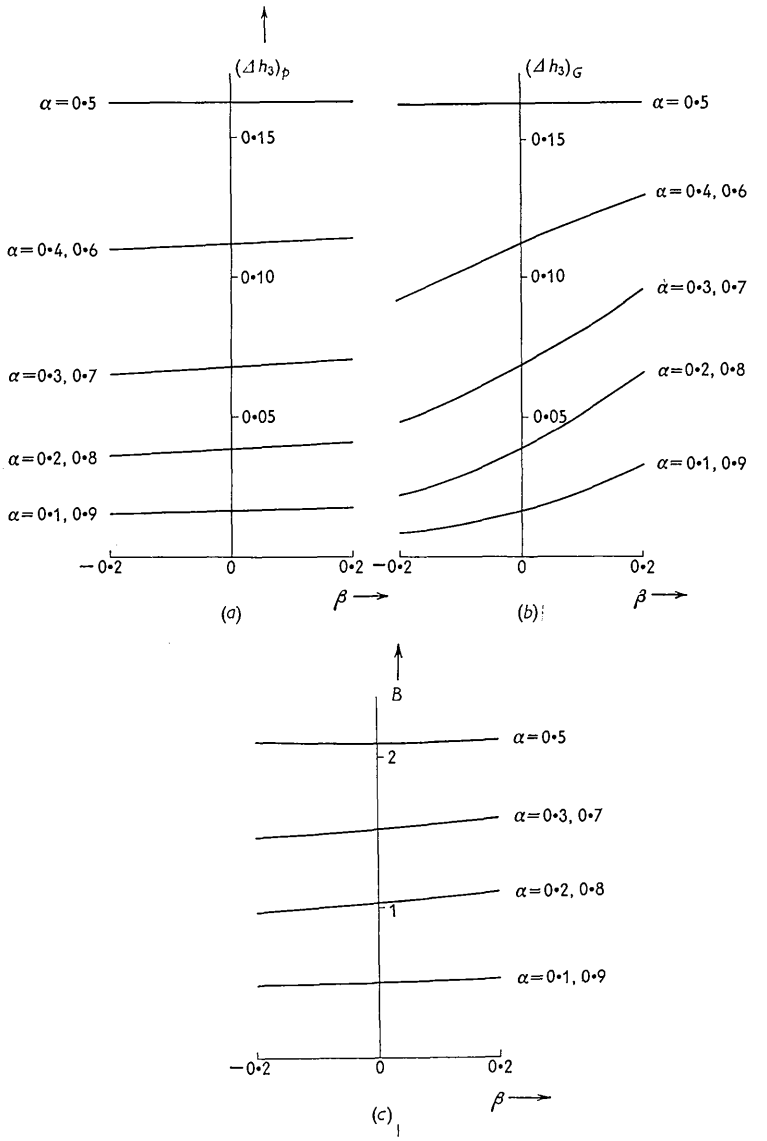

Fig. 4. (*a*) Peak displacement as a function of β for different values of α. The displacement is expressed as a fraction of an order separation. (*b*) Centroid displacement as a function of β for different values of α. The displacement is expressed as a fraction of an order separation. (*c*) Integral breadth B as a function of β for different values of α. B is defined as $\int_0^1 I(h_3)dh_3 \div I_{\max.}$.

$$I(h_3) = 1+2\alpha(1-\alpha)\beta(\beta+2)-2E\cos(2\pi h_3\pm\varepsilon) + 2D\cdot\frac{\cos(4\pi h_3\pm\delta)+Z\cos(2\pi h_3\pm\delta\mp\gamma)}{1+Z^2+2Z\cos(2\pi h_3\pm\gamma)}, \quad (15)$$

where $I(h_3)\equiv I/(f_1^2N\Phi^2)$. In obtaining (15) the assumption has been made that N_m in (6) can be replaced by N: this is a very close approximation provided $\alpha N \gg 1$. In this expression (15) for the dependence of the intensity on the co-ordinate h_3 there are two independent parameters, α and β, which are related to the degrees of faulting and of segregation respectively. The remaining symbols in (15) are defined in terms of α and β by equations (11*a*) and (14*a*). $\beta = 0$ corresponds to the Paterson case of no segregation, and according to Suzuki (1952) β for most alloys will lie well within the range

$$-0{\cdot}2 \leq \beta \leq +0{\cdot}2.$$

For $\alpha = 0{\cdot}5$, (15) simplifies to

$$I(h_3) = \tfrac{1}{4}\beta^2+3(1+\beta+\tfrac{1}{4}\beta^2)/(5+4\cos 2\pi h_3).$$

This represents a symmetrical distribution with maximum intensity at half-integral values of h_3, just as for the case of no segregation.

If $\alpha \neq 0{\cdot}5$, segregation gives rise to a change in the positions of the diffraction peaks, an asymmetry

about these positions, and a change in the integral breadths of the diffraction streaks. These effects are illustrated in Fig. 3, which shows the shape of the reflexions for $\alpha = 0{\cdot}25$, $\beta = 0$ (faulting without segregation) and for $\alpha = 0{\cdot}25$, $\beta = 1{\cdot}0$ (faulting with segregation). (The value $\beta = 1{\cdot}0$ is well outside the likely range of β: it is chosen here to make the asymmetry of the diffraction peak in Fig. 3 immediately obvious). In the former case faulting displaces the peak from 0 to P_1 and broadens the reflexion symmetrically, whereas segregation displaces the peak further (to P_2) and makes the reflexion asymmetrical, so that the centroid is at G, where $OG > OP_2$.

With the aid of the Harwell Mercury computer the values of OP_2 and OG (expressed as fractions of the order separation) and of the integral breadth B were evaluated from (15) for different combinations of α, β. The results are given in Figs. 4(*a*), (*b*), (*c*) for the ranges $0 \leq \alpha \leq 1$, $-0{\cdot}2 \leq \beta \leq 0{\cdot}2$; the curves are the same for α, $1-\alpha$ and for $3M+1$, $3M-1$ reflexions, as indicated by (15) which is unchanged (except for the sign of h_3) when α is replaced by $1-\alpha$ or $\pm$ by $\mp$. These curves show that the position of the centroid of a reflexion is much more sensitive to a change in β than the peak position or the integral breadth. Thus for $\alpha = 0{\cdot}1$, $\beta = 0$ the centroid and peak position are equally displaced by a given amount; if now β increases to 0·1 the peak displacement and integral breadth change by an additional 2%, whereas the centroid is displaced by a further 50%.

We conclude that as far as single crystal diffraction patterns are concerned the principal changes induced by segregation are the introduction of weak diffuse streaks between reflexions in the columns having $H_1-H_2 = 3M$, and of asymmetry in the remaining reflexions. These effects are shown schematically in Fig. 5 for the case $\beta > 0$; for $\beta < 0$ the asymmetry is reversed, the centroid displacement being less than the peak displacement.

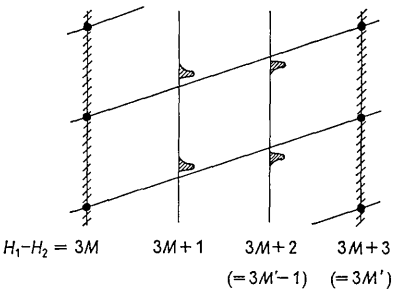

Fig. 5. Schematic diagram showing principal changes in reciprocal lattice induced by segregation. In the $3M$ columns of reflexions a diffuse intensity band appears, while the reflexions in the $3M \pm 1$ columns are broadened asymmetrically.

Fig. 6. Effect of combined faulting and segregation on the profiles of powder diffraction lines up to {400}.

3. Powder pattern

(*a*) *General*

The effect of combined faulting and segregation on the powder diffraction pattern can be determined in the way indicated by Paterson (1952). The value of H_1-H_2 for each component of an $\{hkl\}$ line is found from equation (1*a*); if $H_1-H_2 = 3M$ this component is sharp and undisplaced, whereas if $H_1-H_2 = 3M \pm 1$ the component is broadened asymmetrically and displaced to higher or lower Bragg angles, according to the sign $\pm$. Fig. 6 shows diagrammatically the appearance of the powder pattern up to {400}.

{311} is broadened symmetrically, as it contains an equal number of components of the types $3M+1$ and $3M-1$; and for the same reason its change of integral breadth, as induced by segregation, is much greater than for the other lines.

The peak displacement $(\Delta 2\theta)_p$ of the component of a powder line is related to $(\Delta h_3)_p$ by the equation (Warren & Warekois, 1955):

$$(\Delta 2\theta)_p = 2 \tan\theta \cos^2\varphi (\Delta h_3)_p / h_3 , \qquad (16)$$

where θ is the Bragg angle and φ the angle between the vectors $\mathbf{B}_3$ and $H_1\mathbf{B}_1+H_2\mathbf{B}_2+H_3\mathbf{B}_3$. For $\alpha \ll 1$, the same form of equation applies to the centroid displacement:

$$(\Delta 2\theta)_G = 2 \tan\theta \cos^2\varphi (\Delta h_3)_G / h_3 . \qquad (16a)$$

As $(\Delta h_3)_p$ is relatively insensitive to changes of β (§ 2(*d*)), the faulting parameter, α, can be deduced from the observed $(\Delta 2\theta)_p$, using (16) and Fig. 4(*a*) and assuming $\beta = 0$. β can then be found from the observed $(\Delta 2\theta)_G$, using (16*a*) and Fig. 4(*b*).

(*b*) *Particular applications*

It is clear that in looking for segregation effects we must choose alloys with values of β as high as possible. β increases with the difference in stacking fault energies and with the difference in atomic scattering factors of the alloy components, and it is preferable to choose an intermediate composition of an alloy with a wide solid solution range (Suzuki, 1952). Stacking fault measurements by diffraction methods have been reported on 50/50 Ag–Au (Smallman & Westmacott, 1957) and on 50/50 Co–Ni (Christian & Spreadborough, 1957); from Suzuki's theory and estimates of stacking fault energies by Thornton & Hirsch (1958) β would be about 0·03 for X-ray scattering from Ag–Au and about 0·1 for neutron scattering from Co–Ni. It is possible that segregation could be detected in these cases by comparing the shapes of the three types of line (Fig. 6) represented by {111}, {200} and {311}.

APPENDIX

The treatment in § 2 can be extended to allow for the change of layer spacing accompanying segregation. Let A_3, $A_3(1+\varepsilon/2\pi)$, $A_3(1+\varepsilon/\pi)$ be the spacings between layers with average scattering factors of f_1 and f_1, f_1 and f_2, f_2 and f_2. It is easily shown that formula (15) for the intensity of the $3M\pm1$ reflexions is then modified, assuming $\varepsilon \ll 1$, to

$$I(h_3) = 1+2\alpha(1-\alpha)\beta(\beta+2)-2S\cos(2\pi h_3+s) + \tfrac{1}{2}T\cdot\frac{\cos(4\pi h_3+t)+P\cos(2\pi h_3+t-p)}{1+P^2+2P\cos(2\pi h_3+p)}, \quad (17)$$

where

$$\begin{aligned}
S\cos s &= \tfrac{1}{2}+\tfrac{1}{2}\alpha(1-\alpha)\beta(4+\beta) \pm\sqrt{3}\alpha(1-\alpha)(1-2\alpha)\beta(1+\beta)\varepsilon h_3,\\
S\sin s &= \pm\tfrac{1}{2}\sqrt{3}(1-2\alpha)(1-\alpha\beta^2+\alpha^2\beta^2) +\alpha(1-\alpha)(1+\beta)(2+\beta)\varepsilon h_3;\\
Q\cos q &= 1-2\alpha+2\alpha^2\mp\sqrt{3}\alpha(1-\alpha)(1-2\alpha)\varepsilon h_3,\\
Q\sin q &= \pm\sqrt{3}(1-2\alpha)+\alpha(1-\alpha)\varepsilon h_3;\\
R\cos r &= -1\mp\tfrac{1}{2}\sqrt{3}(1-2\alpha)\varepsilon h_3,\\
R\sin r &= -\tfrac{3}{2}\varepsilon h_3;\\
P\cos p &= \tfrac{1}{2},\\
P\sin p &= \pm\tfrac{1}{2}\sqrt{3}(1-2\alpha)+2\alpha(1-\alpha)\varepsilon h_3;\\
T\cos t &= Q^2\cos 2q-4\alpha(1-\alpha)(1+\beta)QR\cos(q+r) +4\alpha^2(1-\alpha)^2(1+\beta)^2R^2\cos 2r,\\
T\sin t &= Q^2\sin 2q-4\alpha(1-\alpha)(1+\beta)QR\sin(q+r) +4\alpha^2(1-\alpha)^2(1+\beta)^2R^2\sin 2r.
\end{aligned}$$

For a given alloy, with finite values of α, β and ε, the profiles of the $3M+1$ and $3M-1$ reflexions are no longer equivalent; moreover, these profiles are different for the successive peaks occurring with increasing h_3. Evaluation of (17) with the aid of the Mercury computer for the case $\varepsilon = 0{\cdot}02$ showed that the values of the points on the curves in Figs. 4(*a*) and 4(*b*) (corresponding to $\varepsilon = 0$) were changed by about 7% for the first order peak and 22% for the second order peak. For many alloys, in particular those such as Ag–Au and Co–Ni with a wide range of solid solution, ε is practically zero and the simpler theory of S_2 is then adequate.

Thanks are due to Mr T. M. Valentine and Mr T. Vann for handling the bulk of the calculations.

References

CHRISTIAN, J. W. & SPREADBOROUGH, J. (1957). *Proc. Phys. Soc.* B, **70**, 1151.

COTTRELL, A. H. (1954). 'Relation of Properties to Microstructure'. A.S.M. Symposium Report, 131.

PATERSON, M. S. (1952). *J. Appl. Phys.* **23**, 805.

SMALLMAN, R. E. & WESTMACOTT, K. H. (1957). *Phil. Mag.* (8), **2**, 669.

SUZUKI, H. (1952). *Sci. Reports Res. Inst. Tohoku Univ.* A, **4**, 455.

THORNTON, P. R. & HIRSCH, P. B. (1958). *Phil. Mag.* (8), **3**, 738.

WARREN, B. E. & WAREKOIS, E. P. (1955). *Acta Metallurg.* **3**, 473.

WILLIS, B. T. M. (1958). *Proc. Roy. Soc.* A, **248**, 183.

Acta Cryst. (1959). **12**, 689

The Crystal Structures of $PuNi_3$ and $CeNi_3$*

BY DON T. CROMER AND CLAYTON E. OLSEN

University of California, Los Alamos Scientific Laboratory, Los Alamos, New Mexico, U.S.A.

(*Received* 9 *December* 1958)

The structure of $PuNi_3$ and the structure and composition of $CeNi_3$ have been determined by single crystal X-ray methods. $PuNi_3$ has three formula units in a rhombohedral unit cell with $a = 6{\cdot}22$ Å and $\alpha = 33°\ 44'$, probable space group $R\bar{3}m$. $CeNi_3$ has six formula units in a hexagonal cell with $a = 4{\cdot}98$ and $c = 16{\cdot}54$ Å, probable space group $P6_3/mmc$. These structures are both derived from stacking single layers of the MNi_5 structure ($CaCu_5$-type) and double layers of the MNi_2 structure (Cu_2Mg-type).

Introduction

Because of the many similarities between the plutonium–nickel and cerium–nickel binary phase diagrams, structures of compounds in these two systems are simultaneously being investigated. The plutonium–nickel phase diagram, published originally by Wensch & Whyte (1951), shows the existence of the compounds PuNi, $PuNi_2$, $PuNi_3$, $PuNi_4$, $PuNi_5$ and Pu_2Ni_{17}. The structures of $PuNi_2$, $PuNi_5$ and Pu_2Ni_{17} have been reported in a review by Coffinberry & Ellinger (1956) to be of the Cu_2Mg, $CaCu_5$ and Th_2Ni_{17} structure types, respectively. Vogel (1947), in a study of the cerium–nickel phase diagram, lists the compounds Ce_3Ni,

* Work performed under the auspices of the Atomic Energy Commission.